Biochimica et Biophysica Acta 1852 (2015) 1242–1252

Contents lists available at ScienceDirect

Biochimica et Biophysica Acta

journal homepage: www.elsevier.com/locate/bbadis

Role of fibroblast growth factor 21 in the early stage of NASH induced by methionine- and choline-deficient diet☆,☆☆

Naoki Tanaka [a,b], Shogo Takahashi [a], Yuan Zhang [c], Kristopher W. Krausz [a], Philip B. Smith [d], Andrew D. Patterson [d], Frank J. Gonzalez [a,*]

[a] Laboratory of Metabolism, Center for Cancer Research, National Cancer Institute, National Institutes of Health, Bethesda, MD, United States
[b] Department of Metabolic Regulation, Shinshu University Graduate School of Medicine, Matsumoto, Japan
[c] Department of Pharmacology, UT Southwestern Medical Center, Dallas, TX, United States
[d] Department of Veterinary and Biomedical Sciences and the Center for Molecular Toxicology and Carcinogenesis, The Pennsylvania State University, University Park, PA, United States

ARTICLE INFO

Article history:
Received 19 November 2014
Received in revised form 18 February 2015
Accepted 24 February 2015
Available online 28 February 2015

Keywords:
ER stress
Lipotoxicity
ATGL
PGC1α
PPARα

ABSTRACT

Fibroblast growth factor 21 (FGF21) is a modulator of energy homeostasis and is increased in human nonalcoholic liver disease (NAFLD) and after feeding of methionine- and choline-deficient diet (MCD), a conventional inducer of murine nonalcoholic steatohepatitis (NASH). However, the significance of FGF21 induction in the occurrence of MCD-induced NASH remains undetermined. C57BL/6J *Fgf21*-null and wild-type mice were treated with MCD for 1 week. Hepatic *Fgf21* mRNA was increased early after commencing MCD treatment independent of peroxisome proliferator-activated receptor (PPAR) α and farnesoid X receptor. While no significant differences in white adipose lipolysis were seen in both genotypes, hepatic triglyceride (TG) contents were increased in *Fgf21*-null mice, likely due to the up-regulation of genes encoding CD36 and phosphatidic acid phosphatase 2a/2c, involved in fatty acid (FA) uptake and diacylglycerol synthesis, respectively, and suppression of increased mRNAs encoding carnitine palmitoyl-CoA transferase 1α, PPARγ coactivator 1α, and adipose TG lipase, which are associated with lipid clearance in the liver. The MCD-treated *Fgf21*-null mice showed increased hepatic endoplasmic reticulum (ER) stress. Exposure of primary hepatocytes to palmitic acid elevated the mRNA levels encoding DNA damage-inducible transcript 3, an indicator of ER stress, and FGF21 in a PPARα-independent manner, suggesting that lipid-induced ER stress can enhance hepatic FGF21 expression. Collectively, FGF21 is elevated in the early stage of MCD-induced NASH likely to minimize hepatic lipid accumulation and ensuing ER stress. These results provide a possible mechanism on how FGF21 is increased in NAFLD/NASH.

Published by Elsevier B.V.

1. Introduction

Fibroblast growth factor 21 (FGF21), discovered in 2000, is a protein consisting of 210 and 209 amino acids in mouse and humans, respectively [1,2]. While FGF21 is mainly synthesized in liver and secreted into blood, the pancreas, adipose tissue, and stressed muscle may also be sources of FGF21 production [3–7]. Circulating FGF21 binds to a plasma membrane receptor complex, mainly FGF receptor 1 and β-Klotho, and enhances expression of glucose transporter 1 in extra-hepatic tissues, such as adipose tissues, leading to improvement of systemic insulin sensitivity [8,9]. Recombinant FGF21 injection markedly decreases plasma glucose, fatty acid (FA), and triglycerides (TG) in diabetic rhesus monkeys [10,11], and treatment with LY2405319, a recombinant variant of FGF21, causes significant improvement in dyslipidemia in obese humans with type 2 diabetes [12]. Therefore, FGF21 is a potent modulator of glucose/lipid metabolism.

Fgf21 mRNA level is mainly regulated in the liver by several transcription factors associated with energy homeostasis. Peroxisome proliferator-activated receptor (PPAR) α is a ligand-activated nuclear receptor expressed in the liver that regulates lipid homeostasis-

Abbreviations: ALT, Alanine aminotransferase; APAP, Acetaminophen; ATGL, Adipose triglyceride lipase; BAT, Brown adipose tissue; BW, Body weight; DAG, Diacylglycerol; EGR1, Early growth response 1; ER, Endoplasmic reticulum; FA, Fatty acid; FGF, Fibroblast growth factor; FXR, Farnesoid X receptor; HBSS, Hank's buffered salt solution; H_2O_2, Hydrogen peroxide; HSL, Hormone-sensitive lipase; JNK, c-Jun N-terminal kinase; MCD, Methionine- and choline-deficient diet; MCS, Methionine- and choline-supplemented MCD (control) diet; MS, Mass spectrometry; NAFLD, Nonalcoholic fatty liver disease; NASH, Nonalcoholic steatohepatitis; OA, Oleic acid; PA, Palmitic acid; PBS, Phosphate-buffered saline; PGC, Peroxisome proliferator-activated receptor gamma coactivator; PPAR, Peroxisome proliferator-activated receptor; qPCR, Quantitative polymerase chain reaction; TG, Triglyceride; TNF, Tumor necrosis factor; WAT, White adipose tissue

☆ **Potential conflict of interest:** The authors have declared that no conflict of interest exists.

☆☆ **Financial support:** This study was supported by the National Cancer Institute Intramural Research Program and U54 ES16015 (F.J.G) and ES022186 (A.D.P).

* Corresponding author at: Laboratory of Metabolism, Center for Cancer Research, National Cancer Institute, National Institutes of Health, Bethesda, MD 20892, United States. Tel.: +1 301 496 9067; fax: +1 301 496 8419.
E-mail address: gonzalef@mail.nih.gov (F.J. Gonzalez).

http://dx.doi.org/10.1016/j.bbadis.2015.02.012
0925-4439/Published by Elsevier B.V.

associated genes [13]. FGF21 is significantly increased in wild-type mice treated with PPARα activators, such as Wy-14,643 and fibrates, but not in similarly-treated *Ppara*-null mice [14,15]. Additionally, constitutional levels of hepatic *Fgf21* mRNA and serum FGF21 were significantly lower in *Ppara*-null mice compared with the wild-type mice [14,15]. These findings indicate a critical role for PPARα in regulating FGF21 expression. While fasting and a ketogenic diet are strong physiological inducers of FGF21 in mice, induction was detected even in *Ppara*-null mice to some degree [14,16], thus suggesting that factors other than PPARα may contribute to the increase of FGF21 expression. Activation of farnesoid X receptor (FXR) and protein kinase A signaling can also up-regulate hepatic FGF21 expression [5,17–19].

Since FGF21 is synthesized in hepatocytes, it is natural to consider that FGF21 is influenced by pathological changes in the liver. For example, hepatic *Fgf21* mRNA and serum FGF21 levels were robustly increased after acetaminophen (APAP) administration in mice, and co-administration of recombinant FGF21 with APAP ameliorated hepatotoxicity through attenuating oxidative stress [20]. Additionally, *Fgf21*-null mice had an increase in lipopolysaccaride-induced liver injury and co-treatment of recombinant FGF21 partially improved the survival [21]. These findings indicate hepatoprotective properties of FGF21, but the role of FGF21 induction in chronic liver diseases is incompletely understood.

Nonalcoholic fatty liver disease (NAFLD) is one of the major causes of persistent liver abnormalities increasing worldwide. Due to excess calorie intake and sedentary lifestyle, surplus lipids are stored in hepatocytes, a condition designated as hepatic steatosis. Nonalcoholic steatohepatitis (NASH) may develop through increasing hepatic inflammation and/or hepatocyte damage to steatotic liver, leading to hepatic fibrosis, hepatocellular carcinoma, and eventually death [22–24]. Hepatic *Fgf21* mRNA and serum FGF21 are elevated in human NAFLD and correlated with the degree of steatosis [25–28], but the mechanism by which FGF21 is induced in steatotic hepatocytes and its role in hepatic steatosis are not known.

Treatment with a methionine- and choline-deficient diet (MCD) is a conventional and useful model to induce NASH in rodents. While hepatic *Fgf21* mRNA and serum FGF21 were robustly increased after 2-week MCD feeding [29], the significance of FGF21 induction in the early stage of MCD-induced NASH (MCD-NASH) remains unclear. In the present study, MCD was used to treat *Fgf21*-null and wild-type mice for 1 week and the phenotypical changes were examined. The livers of *Fgf21*-null mice revealed greater TG accumulation and endoplasmic reticulum (ER) stress compared with their wild-type counterparts in the early stage of MCD-NASH. *In vitro* studies using mouse primary hepatocytes uncovered that ER stress and oxidative stress augmented the mRNA levels of *Fgf21*. Additionally, treatment of mouse primary hepatocytes with palmitic acid (PA) induced the expression of *Fgf21* in a PPARα-independent manner, and the increase was likely associated with increased DNA damage-inducible transcript 3 (*Ddit3*, also designated as CHOP), a typical indicator of ER stress. Collectively, FGF21 was induced in the early stage of MCD-NASH in response to lipid accumulation likely in order to moderate lipid-derived ER stress. These results shed new insights into the physiological role of FGF21 and a possible mechanism of FGF21 induction in the pathogenesis of NAFLD/NASH.

2. Methods

2.1. Mice and treatment

All studies were conducted according to Institute of Laboratory Animal Resource guidelines and approved by the National Cancer Institute Animal Care and Use Committee. The mice were housed in a specific pathogen-free environment controlled for temperature and light (25 °C, 12-h light/dark cycle) and maintained with NIH31 regular chow and tap water *ad libitum*. The MCD was purchased from Dyets Inc. (#58810; Bethlehem, PA) and methionine- and choline-supplemented MCD diet (MCS, #518754; Dyets) was used as a control diet. The compositions of these diets were described previously [29,30]. Before starting the experiments, regular chow was replaced with MCS for acclimatization. After acclimatization for 3–5 days, the mice were weighed and moved to new cages and the respective diet was given. To check the expression of *Fgf21* mRNA, 8- to 12-week-old male C57BL/6NCr mice were treated with MCD or control MCS for 1 week (n = 7–8/group) and the liver, epididymal, inguinal, and perirenal white adipose tissue (WAT), and interscapular brown adipose tissue (BAT) harvested. Additionally, 16- to 18-week-old male C57BL/6NCr mice were similarly treated with MCD or control MCS for 1 week (n = 6–9/group), and mRNA levels in liver and pancreas measured. Liver samples of mice after 3-day, 1-week, and 2-week MCD treatment used in a previous study [30] were also examined as the time-course assay (n = 5/group). In order to investigate the contribution of PPARα and FXR to the hepatic *Fgf21* mRNA induction, MCD or control MCS was fed to male 8- to 12-week-old wild-type, *Ppara*-null, and *Fxr*-null mice for 2 weeks (n = 4–5/group). To determine the significance of FGF21 induction in the occurrence of MCD-NASH, MCD or MCS was given to male 6- to 10-week-old wild-type or *Fgf21*-null mice on C57BL/6J genetic background [31] for 1 week (n = 5/group). In all experiments, mice were weighed and killed after a 6-h fasting. Blood was collected using Serum Separator Tubes (Becton, Dickinson and Company, Franklin Lakes, NJ) and centrifuged for 10 minutes at 8,000 *g* at 4 °C for obtaining serum. Liver and epididymal WAT were harvested, weighed, and divided into the two parts. One part of these tissues was immediately soaked in 10% neutral formalin for histological examination. Sera and the remaining tissues were immediately frozen in liquid nitrogen and kept at −80 °C until use.

2.2. Isolation and treatment of mouse primary hepatocytes

Mouse primary hepatocytes were isolated from C57BL/6NCr wild-type and *Ppara*-null mice at the age of 8 to 12 weeks [32]. Briefly, the abdomen was incised under anesthesia and mesentery and intestine were moved to expose the portal vein. A cannula was inserted into the portal vein and liver was perfused with 40 ml of Hank's buffered salt solution (HBSS) without magnesium or calcium (Gibco, Carlsbad, CA) containing 1 mM EDTA at 4 ml/min. Blood was extravasated by cutting the inferior vena cava. After perfusion of the entire liver using 50 ml of HBSS containing collagenase I and II (0.6 mg/ml each, Gibco) and calcium chloride dehydrate (5 mM) at the speed of 6 ml/min, the digested liver was removed and placed in a sterile 10-cm Petri dish with 0.01 M phosphate-buffered saline (PBS). The hepatic capsule was torn by fine-tip forceps and dispersed cells were filtered through 70-μm cell strainer (BD Biosciences, Sparks, MD) into a 50-ml tube and centrifuged at 1000 rpm at 4 °C for 3 min. Hepatocytes were further washed and purified by gradient centrifugation using Percoll (GE Healthcare, Piscataway, NJ). After washing with PBS and trypan blue staining, the number of hepatocytes were counted and then seeded in collagen-coated 12-well plates (BD Biosciences) at a density of 3×10^5 cells/well. Primary hepatocytes were cultured in RPMI 1640 medium (Lonza, Basal, Switzerland) with 10% fetal bovine serum, 2 mM glutamine, and antibiotics (100 U/ml penicillin and 100 μg/ml streptomycin) and treatment started 4–6 h after seeding. To induce ER stress, cells were incubated in RPMI medium containing DMSO (vehicle) or thapsigargin (250 and 500 nM, Sigma-Aldrich, St. Louis, MO) and harvested 6 h after treatment. To induce oxidative stress, cells were incubated in RPMI medium containing sterile distilled water (vehicle) or hydrogen peroxide (H_2O_2, 150 and 300 μM, Sigma-Aldrich) and harvested 4 h after treatment [30]. To determine the response to pro-inflammatory cytokines, cells were treated with RPMI medium containing tumor necrosis factor α (TNFα, 100 ng, Sigma-Aldrich) or the same volume of sterile distilled water for 24 h as described previously [30]. PA and oleic acid (OA), purchased from Sigma-Aldrich, were dissolved in isopropanol at a stock concentration of 40 mM and

added to RPMI medium containing 1% bovine serum albumin based on the methods detailed in previous studies [33,34]. Cells were incubated in RPMI medium containing vehicle, PA (400 μM), or OA (400 μM) and harvested 16 h after treatment. Period of treatment and concentrations of the agents were determined according to cell viability assessed in preliminary experiments. Harvested cells were subjected to determination of mRNA levels.

2.3. mRNA analysis

The mRNA levels were measured by quantitative polymerase chain reaction (qPCR). Total RNA was extracted using a TRIzol Reagent (Invitrogen, Carlsbad, CA) and cDNA was generated from 1 μg RNA with a SuperScript II™ Reverse Transcriptase kit and random oligonucleotides (Invitrogen). Quantitative PCR was performed using SYBR green PCR master mix and ABI Prism 7900HT Sequence Detection System (Applied Biosystems, Foster City, CA) [29,30]. The primer pairs were designed using qPrimerDepot (http://mouseprimerdepot.nci.nih.gov/) and listed in Supplementary Table 1. The mRNA levels were normalized to those of 18S ribosomal RNA and expressed as fold change relative to those of control wild-type mice.

2.4. Histological analysis

Small pieces of liver tissue and epididymal WAT were fixed in 10% neutral formalin, dehydrated by serial ethanol/xylene, and embedded in paraffin. Sections (4-μm thick) were stained by the hematoxylin and eosin method [30] and were evaluated in a blinded manner.

2.5. Biochemical analysis

Serum alanine aminotransferase (ALT) concentrations were measured with an assay kit for ALT (Catachem, Bridgeport, CT) [29,30]. Hepatic TG contents were determined as described previously [29,30] using a kit purchased from Wako Chemicals USA, Inc. (Richmond, VA). For assessment of hepatic oxidative stress, mitochondrial fractions

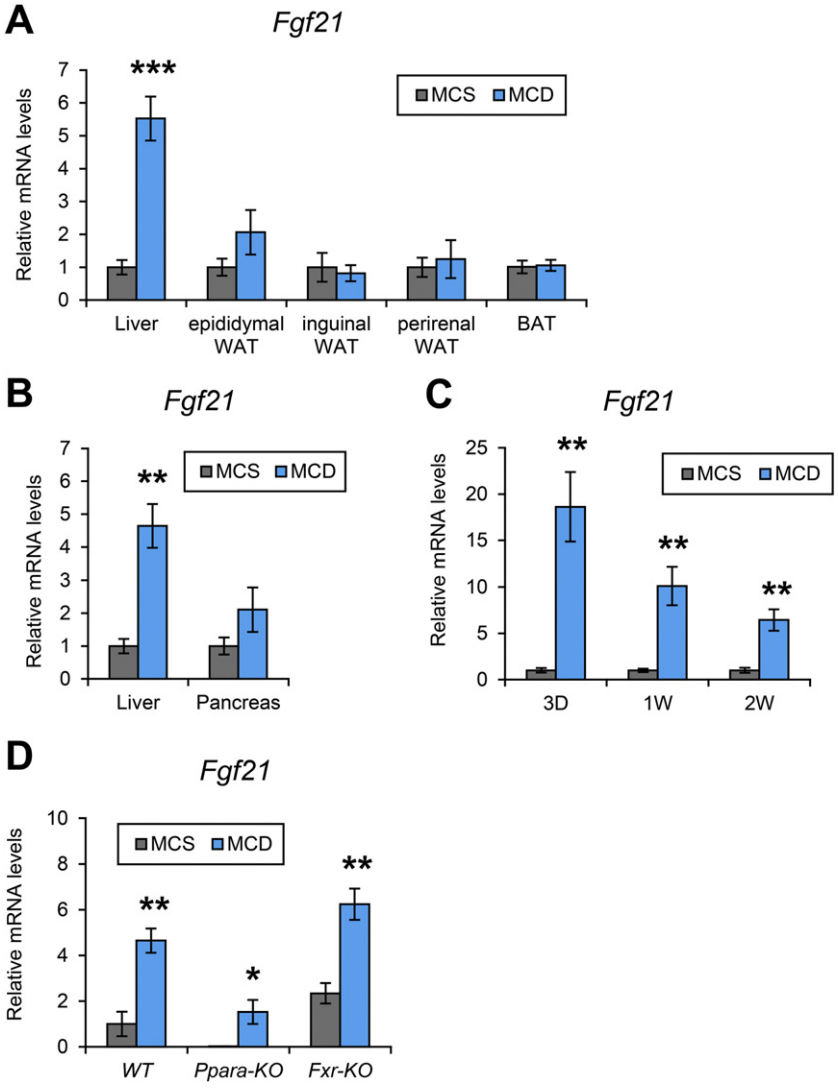

Fig. 1. PPARα-independent induction of FGF21 in the early stage of MCD-NASH. (A) Expression of *Fgf21* mRNA in the liver and white/brown adipose tissue (WAT and BAT, respectively). Male 8- to 12-week-old C57BL/6NCr wild-type mice were fed a methionine- and choline-deficient diet (MCD) or control methionine- and choline-supplemented MCD diet (MCS) for 1 week (n = 7–8/group). The mRNA levels in each tissue were expressed as fold change relative to those of MCS-treated mice. (B) Expression of *Fgf21* mRNA in the liver and pancreas in another mouse set. Male 16- to 18-week-old C57BL/6NCr wild-type mice were fed a MCD or MCS for 1 week (n = 6–9/group). The mRNA levels in each tissue were expressed as fold change relative to those of MCS-treated mice. (C) Time course of hepatic *Fgf21* mRNA induction. Male 8- to 12-week-old C57BL/6NCr wild-type mice were fed a MCD or control MCS for 3 days, 1 week, and 2 weeks (n = 5/group). The mRNA levels of each time point were expressed as fold change relative to those of MCS-treated mice. (D) PPARα- and FXR-independent induction of *Fgf21* by MCD treatment. Male 8- to 12-week-old wild-type, *Ppara*-null, and *Fxr*-null mice were fed a MCD or control MCS for 2 weeks (n = 4–5/group). Values were expressed as fold change relative to those of MCS-treated wild-type mice. Statistical analysis was performed using the Student's *t*-test. $^{*}P < 0.05$, $^{**}P < 0.01$, $^{***}P < 0.001$ vs. MCS-treated mice.

were isolated using 0.25 M sucrose buffer and H_2O_2 levels quantified by PeroxiDetectTM Kit (Sigma-Aldrich). Measurement of protein concentrations was carried out using BSA™ protein assay kit (Thermo Scientific, Rockford, IL).

2.6. Immunoblot analysis

Immunoblot analysis of hormone-sensitive lipase (HSL) and adipose TG lipase (ATGL) was performed as described previously [35]. Briefly, approximately 40 mg of epididymal WAT was homogenized in RIPA buffer containing a proteinase inhibitor cocktail. The homogenates were centrifuged at 10,000*g* for 10 min at 4 °C to obtain lipid-free cytosolic extracts. Cytosolic extracts (30 μg of protein) were subjected to sodium dodecyl sulfate-polyacrylamide gel electrophoresis and transferred to polyvinylidene difluoride membranes. The membranes were blocked with 5% bovine serum albumin or skim milk and incubated overnight with primary antibodies against HSL (Cell Signaling Technology, Inc., Danvers, MA, #4107, 1:1000 dilution), phosphorylated HSL (Cell Signaling, #4139, 1:1000 dilution), ATGL (Cell Signaling, #2439, 1:1000 dilution), and phosphorylated ATGL (Abcam, Cambridge, MA, #135093, 1:1000 dilution). After washing, the blots were incubated with peroxidase-conjugated goat anti-rabbit IgG (Cell Signaling, #7074, 1:3000 dilution) and scanned. The β-actin band was obtained by re-probing the membranes with antibody against β-actin (Abcam, #8227, 1:10,000 dilution) that was used as a loading control.

2.7. Determination of hepatic diacylglycerol (DAG) contents

Approximately 25 mg of liver tissue was homogenized in 300 μl H_2O/400 μl methanol. The homogenates were added to 800 μl of chloroform, incubated at 37 °C while shaking for 20 min, and then centrifuged at 10,000*g* for 20 min. Organic phases were collected, dried, and reconstituted with 100 μl of 1:1 methanol/chloroform. After 50-fold dilution with injection buffer (isopropanol:acetonitrile:H_2O = 2:1:1), samples were subjected to mass spectrometry (MS) analysis. The samples (5 μl) were separated by reverse phase HPLC using a Prominence 20 UFLCXR system (Shimadzu, Columbia, MD) with a Waters (Milford, MA) CSH C18 column (100 mm × 2.1 mm, 1.7 μm particle size) maintained at 55 °C and a 20 min aqueous/acetonitrile/isopropanol gradient, at a flow rate of 225 μl/min. Solvent A was 40% water, 60% acetonitrile with 10 mM ammonium formate, and 0.1% formic acid, and Solvent B was 90% isopropanol, 10% acetonitrile with 10 mM ammonium formate, and 0.1% formic acid. The initial condition was 60% A and 40% B, increasing to 43% B at 2 min, 50% B at 2.1 min, 54% B at 12 min, 70% B at 12.1 min and 99% B at 18 min, and held at 99% B until 20 min before returning to the initial conditions. The eluate was delivered into a

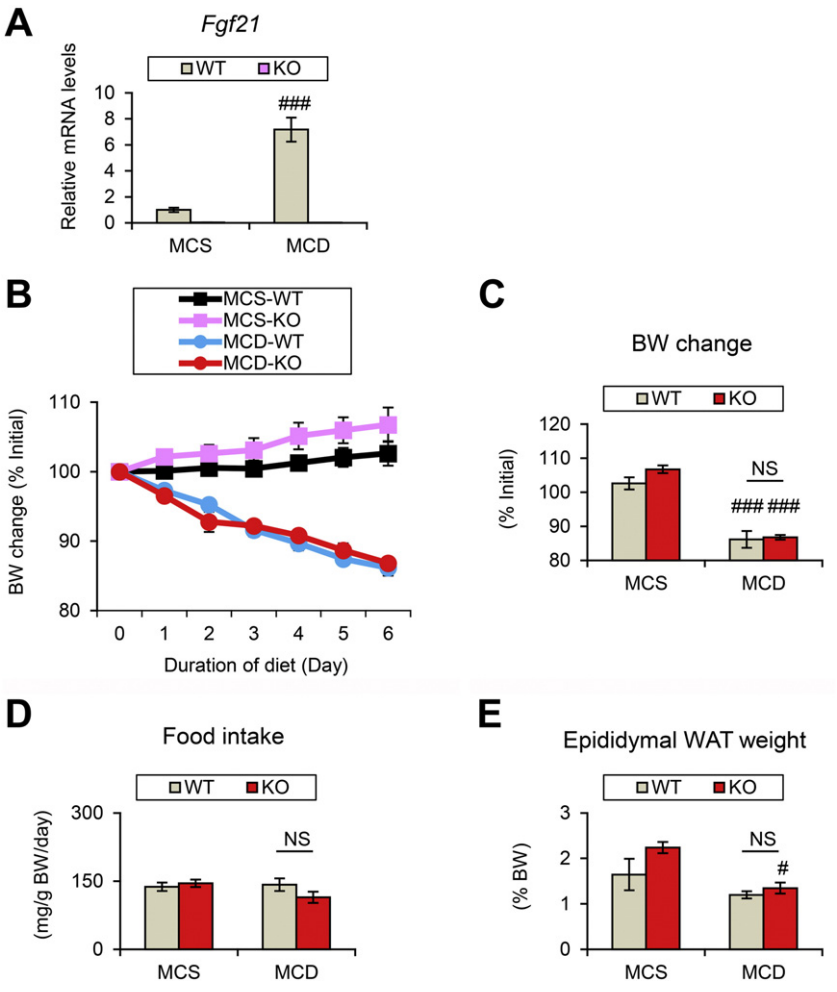

Fig. 2. Similar body weight loss after 1-week MCD treatment in *Fgf21*-null mice. Male 6- to 10-week-old C57BL/6J wild-type (WT) and *Fgf21*-null (KO) mice were treated with a methionine- and choline-deficient diet (MCD) or control methionine- and choline-supplemented MCD diet (MCS) for 1 week (n = 5/group). (A) *Fgf21* mRNA levels. Values were normalized to those of MCS-treated WT mice. (B) Body weight (BW) changes during treatment. (C) BW changes at the end of the treatment. Values were expressed as the percentage relative to BW just before initiating the MCD or MCS treatment. (D) Daily food intake. (E) Weights of epididymal white adipose tissue (WAT). Statistical analysis was performed using the ANOVA test with Bonferroni's correction. $^{\#}P < 0.05$, $^{\#\#\#}P < 0.001$ vs. MCS-treated mice in the same genotype. NS, not significant.

5600 (QTOF) TripleTOF using a Duospray™ ion source (all AB Sciex, Framingham, MA). The capillary voltage was set at 5.5 kV in positive ion mode and 4.0 kV in negative ion mode with a declustering potential of 80 V used in both modes. The mass spectrometer was operated in IDA (Information Dependent Acquisition) mode with a 100 ms survey scan from 100 to 1200 m/z, and up to 20 MS/MS product ion scans (100 ms) per duty cycle using a collision energy of 50 V with a 20 V spread. Hepatic DAG levels were calculated as the sum of DAG 36:1, 36:2, and 36:3, normalized by liver weight, and expressed as fold change relative to those of control wild-type mice.

2.8. Determination of hepatic ceramide contents

Ceramide quantification was carried out as described previously [36] using a Waters Xevo TQ-S triple quadrupole MS system with an Acquity™ I-class UPLC (Waters Corp., Milford, MA). For UPLC, a mixture of A-water, B-acetonitrile/isopropanol (5/2), both containing 10 mM ammonium acetate and 0.1% formic acid was used. Initial 70% A for 1 min, followed by a linear gradient to 50% A at 3 min, to 1% A at 8 min, held until 15 min, returned to the initial conditions over 1 min, and then held for an additional 2 min for column equilibration. The flow rate was 0.4 ml/min and column temperature was maintained at 50 °C. A Waters Xevo TQ-S was operated in MRM mode, with capillary 2.2 kV, source temperature of 150 °C, desolvation gas flow of 850 L/h at 450 °C. The total run time was 18 min, and the cone voltage and collision energy for each of the MRM transitions was determined using Waters IntelliStart™ software.

2.9. Statistical analysis

Quantitative data were expressed as mean ± SEM. Statistical analyses were performed using the two-tailed Student's *t*-test between the two groups, the ANOVA test with Bonferroni's correction among the multiple groups, and the Dunnet's test among the three primary hepatocyte groups, respectively. A p value of less than 0.05 was considered to be statistically significant.

3. Results

3.1. Fgf21 mRNA is increased in the early stage of MCD-NASH independent of PPARα and FXR

MCD treatment for 1 week increased *Fgf21* mRNA levels in liver, but not in epididymal, inguinal, and perirenal WAT and BAT (Fig. 1A). *Fgf21* mRNA was marginally increased in the pancreas after 1 week of MCD treatment, but the increase did not reach statistical significance (Fig. 1B). Increased *Fgf21* mRNA was found up to 3 days after starting MCD treatment (Fig. 1C). Hepatic *Fgf21* mRNA levels were significantly reduced in *Ppara*-null mice compared with wild-type mice on the control diet (approximately 10% of wild-type mice), indicating a major contribution of PPARα to constitutive FGF21 expression. However, the induction of hepatic *Fgf21* mRNA by MCD feeding was also detected in *Ppara*-null and *Fxr*-null mice (Fig. 1D). These results revealed that FGF21 induction in the liver is an early event in MCD-NASH development but occurs independent of PPARα and FXR signaling.

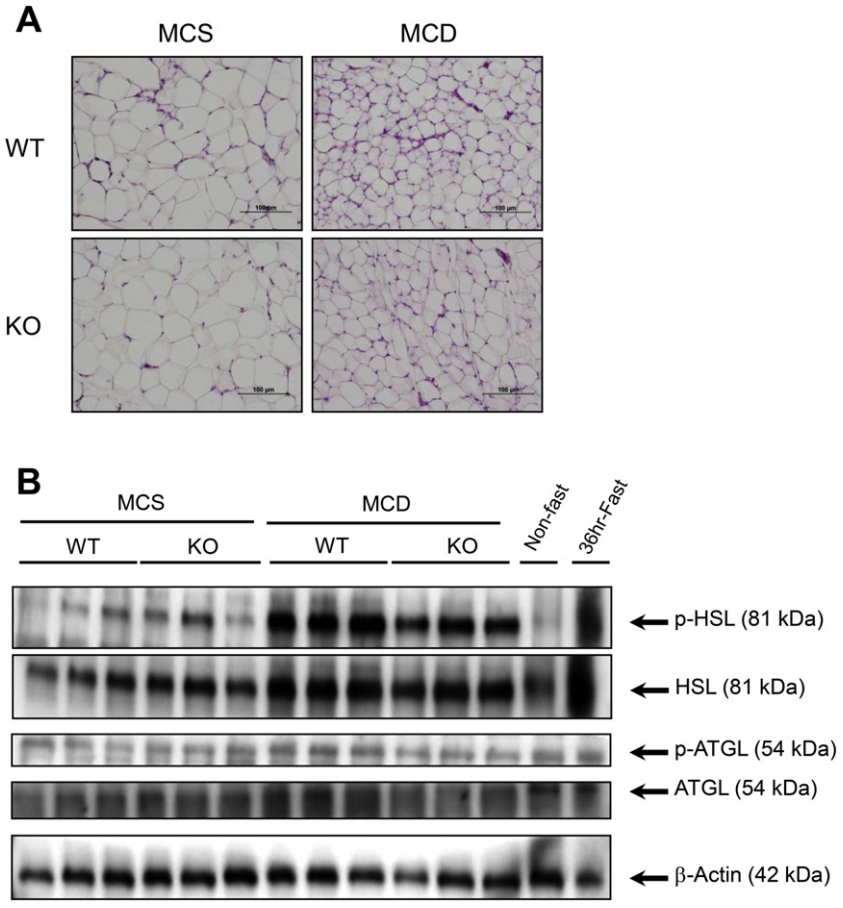

Fig. 3. Similar white adipose lipolysis after 1-week MCD treatment in *Fgf21*-null mice. Epididymal white adipose tissue (WAT) was examined in the same mouse set presented in Fig. 2. WT, wild-type mice; KO, *Fgf21*-null mice. (A) Representative histological appearance of epididymal WAT. Hematoxylin and eosin staining, bar = 100 μm. (B) Immunoblot analysis of phosphorylated and total hormone-sensitive lipase (p-HSL and HSL, respectively) and adipose triglyceride lipase (p-ATGL and ATGL, respectively). Cytosolic extracts of epididymal WAT (30 μg of protein) were loaded in each well. The β-actin band was used as a loading control. Epididymal WAT isolated from a 36 h-fasted mouse was used for detecting the true position of HSL and ATGL bands.

3.2. Body weight loss and enhancement of WAT lipolysis by MCD treatment are not associated with increased FGF21

Body weight (BW) loss and WAT lipolysis appear early after commencing MCD treatment [29]. Since previous studies implied a promoting effect for FGF21 on WAT lipolysis [10,14], anthropometric parameters and WAT phenotypes were examined in *Fgf21*-null mice after 1 week of MCD treatment. Hepatic *Fgf21* mRNA was robustly increased after MCD treatment but was not detected in *Fgf21*-null mice (Fig. 2A). BW changes, food intake, and epididymal WAT mass were not statistically different between MCD-fed wild-type and *Fgf21*-null mice (Fig. 2B–E). Histological appearance of epididymal WAT exhibited a reduction in adipocyte size in both genotypes after MCD treatment (Fig. 3A). Consistently, immunoblot analysis revealed a marked increase in phosphorylated HSL and ATGL in both genotypes by MCD feeding (Fig. 3B); there were no significant changes in the expression of HSL and ATGL between wild-type and *Fgf21*-null mice (Fig. 3B). These results suggest that the enhanced WAT lipolysis after the MCD treatment is not linked with increased FGF21.

3.3. Fgf21-null mice show more severe TG accumulation by MCD treatment

There were no differences in serum ALT concentrations and levels of *Tnf* mRNA, encoding TNFα, and *Cd68* mRNA, which are associated with hepatic inflammation, between the two treated groups (Fig. 4A and C). However, hepatic TG contents were greater in *Fgf21*-null mice compared with the wild-type counterparts after the MCD treatment (Fig. 4D). Histologically, more severe steatosis was found in MCD-treated *Fgf21*-null mice (Fig. 4B).

To examine the mechanism of severe TG accumulation in these mice, the levels of mRNAs encoded by genes involved in FA metabolism were measured. Increases in *Cd36* mRNA, encoding transporter that has an important role in FA uptake from blood into hepatocytes and is down-regulated by FGF21 [9], were noted in MCD-treated *Fgf21*-null mice compared with wild-type mice (Fig. 5A). Carnitine palmitoyl-CoA transferase 1α (*Cpt1a*) mRNA, encoding the first enzyme in mitochondrial β-oxidation, was increased in MCD-fed wild-type mice compared with MCS-fed wild-type mice, but this increase was not observed in *Fgf21*-null mice after MCD feeding (Fig. 5B). There were no significant differences in the mRNAs encoding enzymes associated with FA synthesis, such as fatty acid synthase (*Fasn*), acetyl-CoA carboxylase α (*Acaca*), and stearoyl-CoA desaturase 1 (*Scd1*) between the four mouse groups (Fig. 5C). However, MCD-induced down-regulation of *Scd1* mRNA was apparently milder in the *Fgf21*-null mice compared with wild-type mice ($P = 0.035$ calculated by means of Student's *t*-test, MCD-fed wild-type mice vs. MCD-fed *Fgf21*-null mice), which is in agreement with a previous observation that FGF21 suppresses SCD1 expression in the liver [9].

TG and its precursor DAG are glycerolipids generated from phosphatidate. The mRNA levels of genes associated with phosphatidate-DAG-TG metabolism were also determined. The phosphatidate phosphatase 2a and 2c (*Ppap2a/2c*) mRNAs, involved in DAG synthesis, were increased in MCD-treated *Fgf21*-null mice compared with wild-type mice

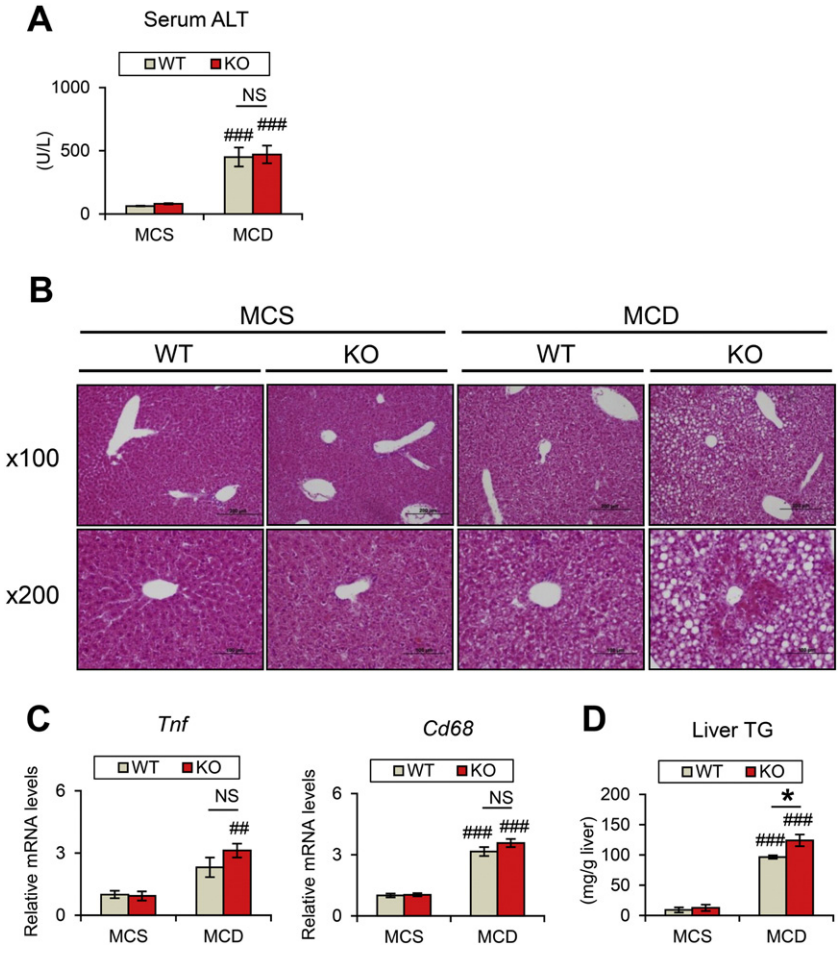

Fig. 4. More severe hepatosteatosis in *Fgf21*-null mice after 1-week MCD treatment. Liver samples were examined in the same mouse set presented in Fig. 2 (n = 5/group). WT, wild-type mice; KO, *Fgf21*-null mice. (A) Serum alanine aminotransferase (ALT) levels. (B) Representative histological appearance of liver. Hematoxylin and eosin staining, bar = 200 μm (×100 magnification) or 100 μm (×200 magnification). (C) qPCR analysis of genes associated with inflammation. The mRNA levels were normalized to those of MCS-treated WT mice. (D) Hepatic triglyceride (TG) contents. Statistical analysis was performed using the ANOVA test with Bonferroni's correction. $^{*}P < 0.05$ between MCD-treated WT and KO mice. $^{\#\#}P < 0.01$, $^{\#\#\#}P < 0.001$ vs. MCS-treated mice in the same genotype. NS, not significant.

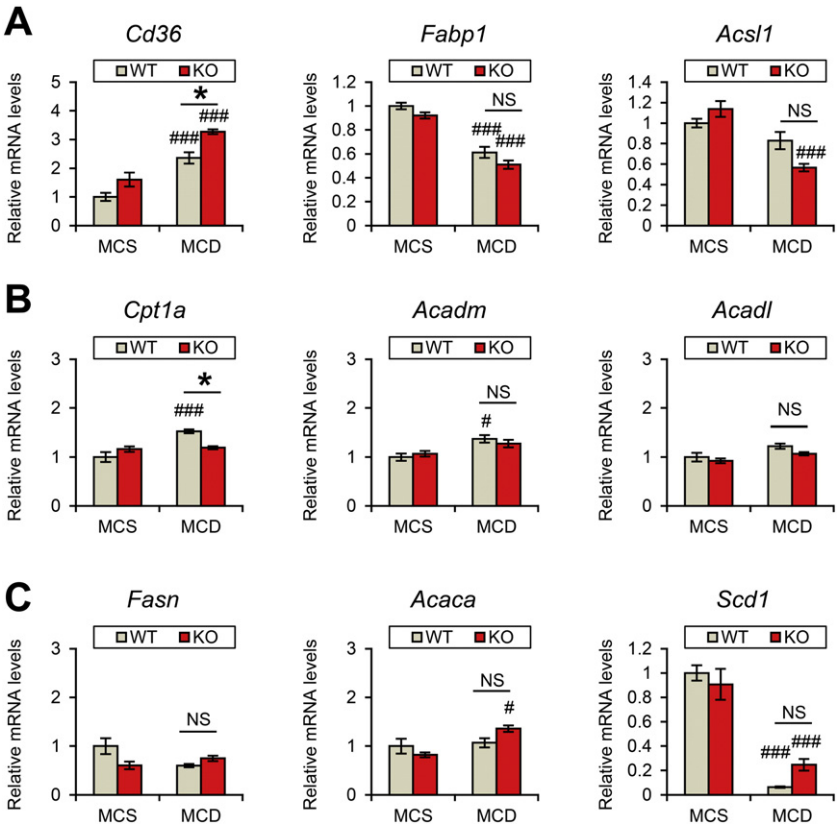

Fig. 5. qPCR analysis of genes associated with fatty acid metabolism. Liver samples obtained from mice used in Fig. 2 were subjected to qPCR analysis (n = 5/group). The mRNA levels of genes involved in fatty acid (FA) uptake and activation (A), mitochondrial β-oxidation (B), and FA synthesis (C) were measured. Values were normalized to those of MCS-treated wild-type (WT) mice. KO, *Fgf21*-null mice. Statistical analysis was performed using the ANOVA test with Bonferroni's correction. $^{*}P < 0.05$ between MCD-treated WT and KO mice. $^{\#}P < 0.05$, $^{\#\#\#}P < 0.001$ vs. MCS-treated mice in the same genotype. NS, not significant.

(Fig. 6A). The expression of DAG acyltransferases 1 and 2 (*Dgat1/2*) mRNAs, TG-synthesizing enzymes, was not changed between the genotypes (Fig. 6A and data not shown). Additionally, *Pnpla2* mRNA encoding ATGL, a major TG-hydrolyzing enzyme in the liver, was increased in MCD-fed wild-type mice compared with MCS-fed wild-type mice, but the increase was not seen in the *Fgf21*-null groups (Fig. 6B). Hepatic contents of DAG and ceramides, active intermediate lipids in FA/glycerolipid cycling, were not different between MCD-treated wild-type and *Fgf21*-null mice (Supplementary Fig. 1).

Among the transcription factors regulating hepatic FA/TG metabolism, greater increases in PPARγ1 (*Pparg1*) mRNA levels were observed in MCD-treated *Fgf21*-null mice (Fig. 6C). Interestingly, *Ppargc1a* mRNA levels encoding PPARγ co-activator 1α (PGC1α), which enhances mitochondrial β-oxidation activity, were increased in MCD-fed wild-type mice, but no increase was found in similarly-treated *Fgf21*-null mice (Fig. 6C). The expression of *Ppara* was similar between the genotypes (Fig. 6C). Overall, increased hepatic TG contents in MCD-treated *Fgf21*-null mice were likely due to up-regulation of *Cd36* and *Ppap2a/2c* and suppression of increased *Cpt1a*, *Pnpla2*, and *Ppargc1a*. While FGF21 did not affect the expression of inflammation-related genes and serum ALT levels in the early stage of MCD-NASH, it played an important role in attenuating hepatic lipid accumulation.

3.4. Fgf21-null mice demonstrate greater ER stress by MCD treatment

Since oxidative stress and ER stress are key components of the pathogenesis of NASH [22–24], these factors were assayed. The levels of mitochondrial H_2O_2 were increased by MCD treatment, but there were no significant differences between the genotypes (Fig. 7A). The levels of NADPH oxidase 2 (*Cybb*) and superoxide dismutase 2 (*Sod2*) mRNAs encoding reactive oxygen species-generating and -eliminating enzyme, respectively, were also similar between the two groups given the MCD (Fig. 7B). However, the *Ddit3*, heat shock protein 5 (*Hspa5*), and tumor necrosis factor receptor superfamily member 10b (*Tnfrsf10b*) mRNAs, representative genes induced by ER stress and ensuing apoptosis, were significantly increased in MCD-treated *Fgf21*-null mice (Fig. 7C).

3.5. PA induces ER stress and FGF21 in mouse primary hepatocytes

The direct association between FGF21 induction, ER stress, and lipid accumulation was explored using mouse primary hepatocytes. Treatment with thapsigargin, a conventional ER stress inducer, augmented *Fgf21* mRNA (Fig. 8A). PA, but not OA, was reported to induce ER stress leading to lipotoxicity in hepatocytes and pancreatic β cells [33,34,37]. Treatment of primary hepatocytes with 400 μM of PA elevated *Ddit3* and *Fgf21* mRNA levels, but treatment with the same concentrations of OA did not (Fig. 8B and C). PA-induced increases in *Fgf21* mRNA were detected even in primary hepatocytes isolated from *Ppara*-null mice (Fig. 8D). These results suggest that PA induces FGF21 in a PPARα-independent manner likely through enhancing ER stress.

3.6. Oxidative stress, but not TNFα, induces FGF21 in mouse primary hepatocytes

Lastly, the contribution of oxidative stress and inflammatory signaling to FGF21 induction was assessed. Treatment of primary hepatocytes with H_2O_2 increased the mRNA levels of *Egr1* encoding early growth response 1 (EGR1), a rapidly-induced transcription factor in response to oxidative stress, and *Fgf21* in a dose-dependent and PPARα-independent manner (Fig. 9A and B). However, treatment with TNFα decreased the *Fgf21* expression (Fig. 9C). These results indicate that FGF21 is induced in response to cellular stresses, rather than TNFα signaling.

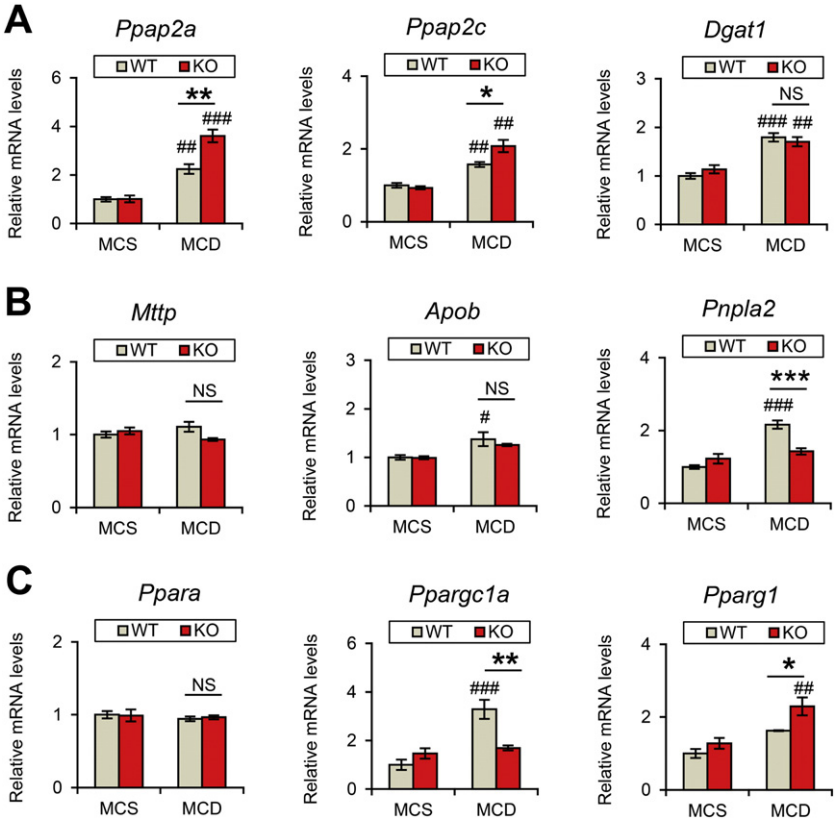

Fig. 6. qPCR analysis of genes associated with glycerolipid metabolism and transcription factors. The same cDNA samples used in Fig. 5 were used (n = 5/group). The mRNA levels of genes associated with triglyceride (TG) synthesis (A), TG secretion or hydrolysis (B), and genes encoding transcription factors (C) were measured. Values were normalized to those of MCS-treated wild-type (WT) mice. KO, *Fgf21*-null mice. Statistical analysis was performed using the ANOVA test with Bonferroni's correction. $^{*}P < 0.05$, $^{**}P < 0.01$, $^{***}P < 0.001$ between MCD-treated WT and KO mice. $^{\#}P < 0.05$, $^{\#\#}P < 0.01$, $^{\#\#\#}P < 0.001$ vs. MCS-treated mice in the same genotype. NS, not significant.

4. Discussion

The present study aimed to explore the role of FGF21 in MCD-NASH. Disruption of *Fgf21* in mice revealed significant increases in hepatic TG and ER stress one week after the MCD treatment. More severe TG accumulation in MCD-fed *Fgf21*-null mice was likely due to increased expression of *Cd36* and *Ppap2a/2c* and suppression of *Cpt1a* and *Pnpla2* expression. Increased *Fgf21* by PA was associated with increased *Ddit3*, but not PPARα activation, in primary hepatocytes. Thus, FGF21 was induced in response to toxic lipid accumulation in the early stage of MCD-NASH possibly to attenuate lipid-derived ER stress (i.e., lipotoxicity). These results demonstrate a critical role for FGF21

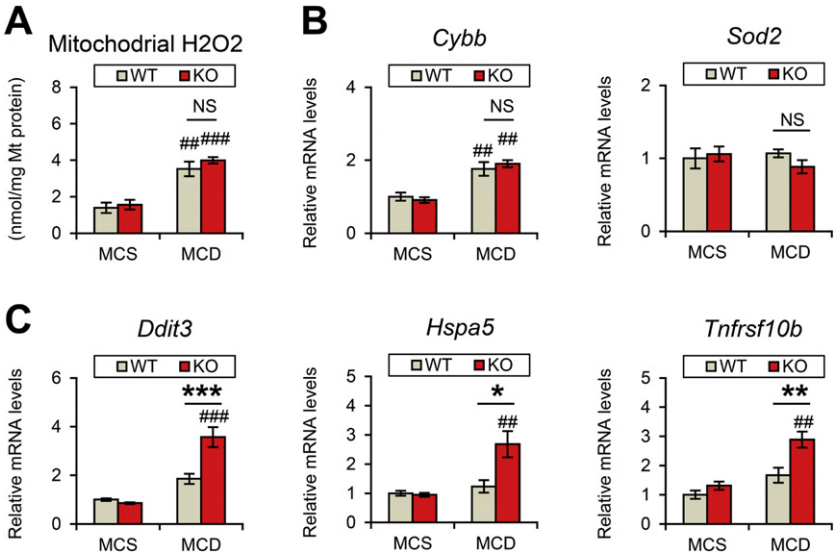

Fig. 7. Greater ER stress in *Fgf21*-null mice after 1-week MCD treatment. Liver samples in the same mouse set presented in Fig. 2 were subjected to assay (n = 5/group). WT, wild-type mice; KO, *Fgf21*-null mice. (A) Mitochondrial H_2O_2 contents. (B and C) qPCR analysis of genes associated with oxidative stress (B), and ER stress (C). Values were normalized to those of MCS-treated WT mice. Statistical analysis was performed using the ANOVA test with Bonferroni's correction. $^{*}P < 0.05$, $^{**}P < 0.01$, $^{***}P < 0.001$ between MCD-treated WT and KO mice. $^{\#\#}P < 0.01$, $^{\#\#\#}P < 0.001$ vs. MCS-treated mice in the same genotype. NS, not significant.

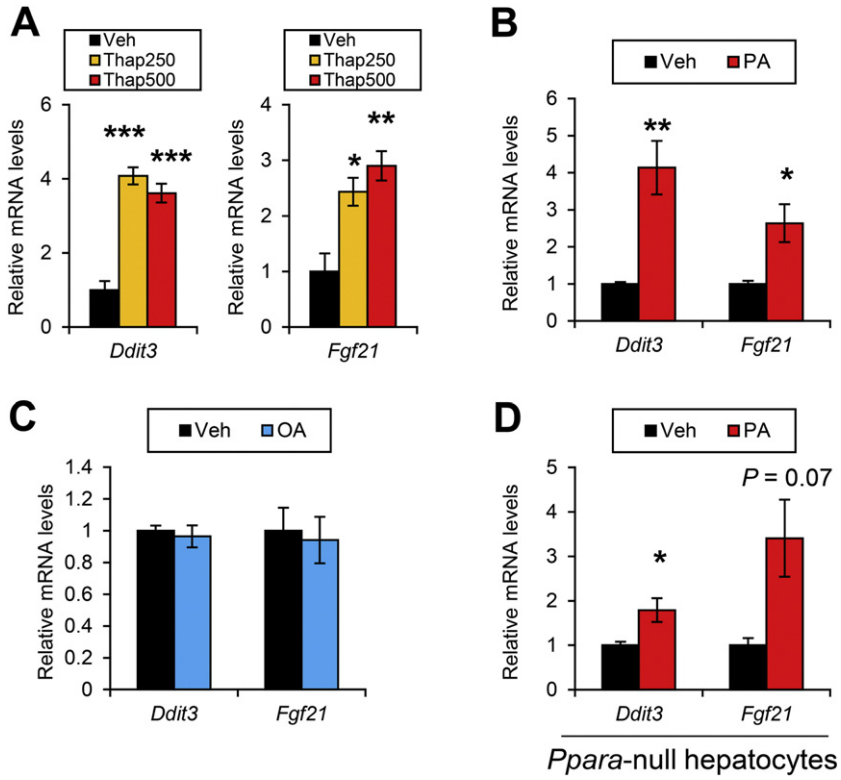

Fig. 8. Palmitate induces *Fgf21* independent of PPARα in mouse primary hepatocytes. (A) Thapsigargin induces ER stress marker *Ddit3* and *Fgf21* mRNAs. Mouse primary hepatocytes were treated with vehicle (Veh) or thapsigargin (Thap, 250 or 500 nM) for 6 h. Statistical analysis was carried out using the Dunnet's test. n = 3–4/group. $^{*}P < 0.05$, $^{**}P < 0.01$, $^{***}P < 0.001$ vs. vehicle-administered hepatocytes. (B and C) Palmitate (PA), but not oleate (OA), induces *Ddit3* and *Fgf21* mRNAs. Mouse primary hepatocytes were treated with vehicle (Veh) or the fatty acid (400 μM) for 16 h. Statistical analysis was conducted using the Student's *t*-test. n = 4–6/group. $^{*}P < 0.05$, $^{**}P < 0.01$ vs. vehicle-administered hepatocytes. (D) PPARα-independent induction of *Fgf21* mRNA by PA. The same experiment as panel (B) was performed using primary hepatocytes isolated from *Ppara*-null mice. Statistical analysis was conducted using the Student's *t*-test. n = 4/group. $^{*}P < 0.05$ vs. vehicle-administered hepatocytes.

in the control of hepatic lipid homeostasis and cellular stress in the context of NAFLD/NASH.

The role of FGF21 on WAT lipolysis is controversial. While some studies reported that FGF21 inhibits lipolysis [38,39], others showed that *Fgf21*-overexpressing mice had smaller white adipocytes and higher lipolysis activity compared with wild-type mice [14]. Additionally, treatment of 3T3-L1 adipocytes with FGF21 induced lipolysis [10], and administration of recombinant FGF21 to mice and monkeys caused reductions in BW and WAT mass [10,11]. In a previous study, elevated *Fgf21* mRNA levels in the liver, increased circulating FGF21, and enhanced WAT lipolysis were found within 2 weeks after commencing MCD treatment [29]. Since WAT lipolysis may promote the development of hepatic steatosis and steatohepatitis [29,40], these observations led to the hypothesis that FGF21 affects the occurrence of MCD-NASH through accelerating WAT lipolysis. However in this study, the extent of WAT lipolysis in MCD-treated *Fgf21*-null mice was similar to wild-type counterparts, suggesting only minor contribution of FGF21 to MCD-induced adipose lipolysis. Recent studies revealed that FGF21 is associated with browning of white adipocytes [41], but a preliminary evaluation found no induction of uncoupling protein 1 and carboxyl ester lipase, typical BAT-specific genes downstream of FGF21 [14], respectively, in the WAT of MCD-treated mice (data not shown). These findings may support the WAT changes observed in the present study.

The livers of MCD-fed *Fgf21*-null mice exhibited lower *Cpt1a* and *Ppargc1a* mRNA levels; these mRNAs encode proteins related to mitochondrial β-oxidation activity, thus indicating delayed FA degradation compared with wild-type mouse livers. This is consistent with the recent observation that hepatic free FA contents were increased and PA degradation in mitochondria (i.e., mitochondrial β-oxidation activity) was decreased in *Fgf21*-null mice fed MCD for 8 weeks [42]. It is also intriguing that *Fgf21* disruption suppressed the up-regulation of *Pnpla2* mRNA in MCD-treated mouse livers. *Pnpla2* encodes ATGL, a key enzyme for TG hydrolysis in the liver [43], and its up-regulation is presumably an adaptive response to rapid and aberrant accumulation of TG in hepatocytes. Thus, lower levels of *Pnpla2* induction may lead to delayed TG turnover. Additionally, higher *Cd36* and *Ppap2a/2c* mRNAs suggest enhanced FA uptake and DAG synthesis in these mice. Therefore, reduced fat clearance and increased TG precursors are possible mechanisms for the higher TG accumulation in MCD-treated *Fgf21*-null mice.

ER is the major site for TG synthesis from FA and phosphatidate/DAG. It is well accepted that saturated FA, such as PA, have pro-apoptotic and cytotoxic properties through inducing ER stress [33,34]. While ER stress was reported to induce FGF21 [44,45], the relationship between ER stress, lipotoxicity, and FGF21 induction are incompletely understood. The present study uncovered PPARα-independent FGF21 induction in response to PA-induced ER stress in mouse primary hepatocytes, in addition to greater TG accumulation and ER stress in MCD-treated *Fgf21*-null mice. These results indicate that endogenous FGF21 might be up-regulated in steatotic hepatocytes in order to protect hepatocytes from increased hepatic lipids and lipid-derived ER stress. Indeed, elevated serum/liver FGF21 was reported in human NAFLD, and significantly correlated severity of steatosis [25–28]. This is presumably an adaptive response to limit fat accumulation and ensuing lipotoxicity. Based on these findings, therapeutic strategies to achieve robust and continuous up-regulation of hepatic FGF21 might be beneficial to treat NAFLD.

The interconnection between ER stress, oxidative stress, and inflammatory signaling leads to hepatocyte injury and progresses steatosis to steatohepatitis. Recently, it was reported that *Fgf21*-null mice exhibited higher levels of serum ALT after MCD feeding for 8 weeks, but not 4 weeks, and increased hepatic TG and malondialdehyde at 8 weeks of MCD treatment [42]. However, these changes might be a consequence of persistent disruption of lipid metabolism and activation of

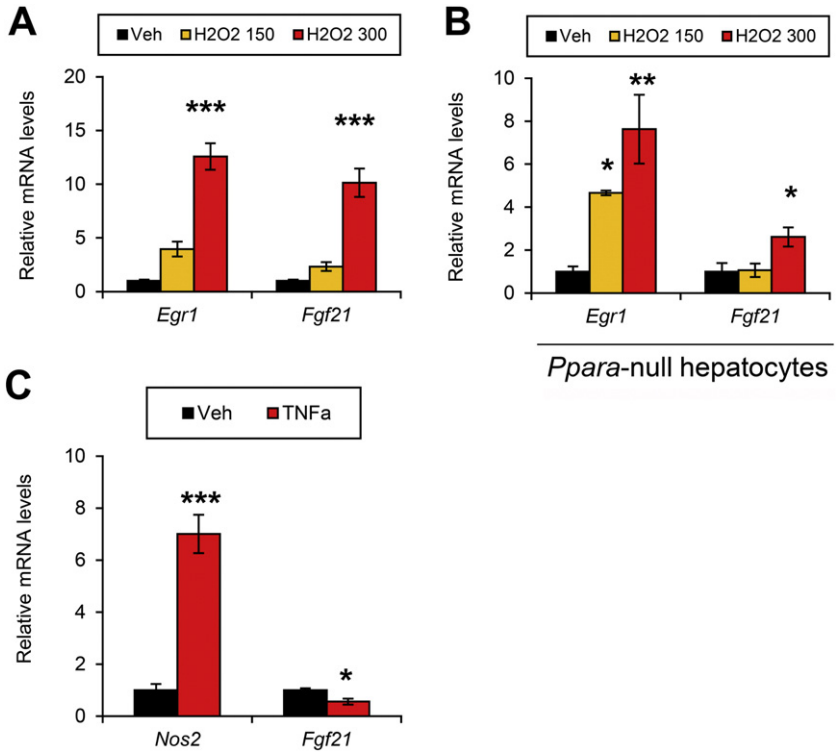

Fig. 9. H_2O_2, but not tumor necrosis factor α, induces *Fgf21* independent of PPARα in mouse primary hepatocytes. (A) H_2O_2 induces oxidative stress-responsive gene *Egr1* and *Fgf21* mRNAs. Mouse primary hepatocytes were treated with vehicle (Veh) or H_2O_2 (150 or 300 μM) for 4 h. Statistical analysis was done using the Dunnet's test. n = 4/group. $^{***}P < 0.001$ vs. vehicle-administered hepatocytes. (B) PPARα-independent induction of *Fgf21* mRNA by H_2O_2. The same experiment as panel (A) was performed using primary hepatocytes isolated from *Ppara*-null mice. Statistical analysis was done using the Dunnet's test. n = 4/group. $^{*}P < 0.05$, $^{**}P < 0.01$ vs. vehicle-administered hepatocytes. (C) Tumor necrosis factor α (TNFα) down-regulates *Fgf21* mRNA. Mouse primary hepatocytes were treated with vehicle (Veh) or TNFα (100 ng) for 24 h. The mRNA levels of *Nos2* (encoding inducible nitric oxide synthase) were used as a positive control. Statistical analysis was conducted using the Student's *t*-test. n = 4–6/group. $^{*}P < 0.05$, $^{***}P < 0.001$ vs. vehicle-administered hepatocytes.

inflammatory cascades, and thus the contribution of FGF21 to early-stage NASH pathologies cannot be assessed in mice under long-term MCD feeding. The present study revealed that, among the factors promoting steatohepatitis, ER stress was singularly enhanced in *Fgf21*-null mice in the early stage of MCD-NASH. This finding indicates that ER stress is associated with up-regulation of FGF21 and increased ER stress is an initial event of progressive MCD-NASH in *Fgf21*-null mice.

This study showed that H_2O_2 can induce *Fgf21* mRNA independent of PPARα in mouse hepatocytes. This result is in accordance with the finding that administration of APAP, a typical oxidative stress inducer, results in robust increases in FGF21 [20]. Furthermore, administration of recombinant FGF21 to *Fgf21*-null mice treated with APAP or MCD attenuated oxidative stress and hepatocyte injury [20,42]. These findings suggest that endogenous FGF21 is up-regulated in diseased livers to protect hepatocytes from oxidative stress.

The mechanism by which cellular stress induces FGF21 deserves further investigation. A recent report demonstrated direct transactivation of FGF21 by ER stress-activated pathways, such as inositol-requiring enzyme 1α-transcription factor X-box binding protein 1 and eukaryotic initiation factor 2α-activating transcription factor 4 axes [45]. Additionally, it was reported that c-Jun N-terminal kinase (JNK) and EGR1 are activated by oxidative stress and the activation is inhibited by FGF21 administration or overexpression [20,46]. Therefore, FGF21 might be up-regulated in response to JNK and EGR1 activation in order to attenuate this activation as a means of feedback inhibition. These observations indicate the possible contribution of stress-activated transcription factors in the induction of FGF21.

In conclusion, the present study uncovered a critical role for FGF21 induction in the early stage of MCD-NASH development that functions to minimize lipid accumulation and ensuing cellular stress in the liver. FGF21 is not only a potent modulator of glucose/lipid metabolism, but also a novel and promising hepatoprotectant.

Transparency Document

The Transparency document associated with this article can be found, in the online version.

Acknowledgments

We thank Linda G. Byrd and John Buckley for providing technical assistance with the mouse studies. This study was supported by the Intramural Research Program, Center for Cancer Research, National Cancer Institute, U554 ES16015 and 1R01ES022186-01, National Institutes of Health.

Appendix A. Supplementary data

Supplementary data to this article can be found online at http://dx.doi.org/10.1016/j.bbadis.2015.02.012.

References

[1] T. Nishimura, Y. Nakatake, M. Konishi, N. Itoh, Identification of a novel FGF, FGF-21, preferentially expressed in the liver, Biochim. Biophys. Acta 1492 (2000) 203–206.
[2] A. Kharitonenkov, A.C. Adams, Inventing new medicines: the FGF21 story, Mol. Metab. 3 (2014) 221–229.
[3] A.C. Adams, T. Coskun, C.C. Cheng, L.S.O. Farrell, S.L. Dubois, A. Kharitonenkov, Fibroblast growth factor 21 is not required for the antidiabetic actions of the thiazoladinediones, Mol. Metab. 2 (2013) 205–214.
[4] F.M. Fisher, S. Kleiner, N. Douris, E.C. Fox, R.J. Mepani, F. Verdeguer, J. Wu, A. Kharitonenkov, J.S. Flier, E. Maratos-Flier, B.M. Spiegelman, FGF21 regulates PGC-1α and browning of white adipose tissues in adaptive thermogenesis, Genes Dev. 26 (2012) 271–281.
[5] E. Hondares, R. Iglesias, A. Giralt, F.J. Gonzalez, M. Giralt, T. Mampel, F. Villarroya, Thermogenic activation induces FGF21 expression and release in brown adipose tissue, J. Biol. Chem. 286 (2011) 12983–12990.

[6] D.V. Chartoumpekis, I.G. Habeos, P.G. Ziros, A.I. Psyrogiannis, V.E. Kyriazopoulou, A.G. Papavassiliou, Brown adipose tissue responds to cold and adrenergic stimulation by induction of FGF21, Mol. Med. 17 (2011) 736–740.
[7] F. Ribas, J. Villarroya, E. Hondares, M. Giralt, F. Villarroya, FGF21 expression and release in muscle cells: involvement of MyoD and regulation by mitochondria-driven signaling, Biochem. J. 463 (2014) 191–199.
[8] A.C. Adams, C. Yang, T. Coskun, C.C. Cheng, R.E. Gimeno, Y. Luo, A. Kharitonenkov, The breadth of FGF21's metabolic actions are governed by FGFR1 in adipose tissue, Mol. Metab. 2 (2013) 31–37.
[9] T. Coskun, H.A. Bina, M.A. Schneider, J.D. Dunbar, C.C. Hu, Y. Chen, D.E. Moller, A. Kharitonenkov, Fibroblast growth factor 21 corrects obesity in mice, Endocrinology 149 (2008) 6018–6027.
[10] A. Kharitonenkov, T.L. Shiyanova, A. Koester, A.M. Ford, R. Micanovic, E.J. Galbreath, G.E. Sandusky, L.J. Hammond, J.S. Moyers, R.A. Owens, J. Gromada, J.T. Brozinick, E.D. Hawkins, V.J. Wroblewski, D.S. Li, F. Mehrbod, S.R. Jaskunas, A.B. Shanafelt, FGF-21 as a novel metabolic regulator, J. Clin. Invest. 115 (2005) 1627–1635.
[11] A. Kharitonenkov, V.J. Wroblewski, A. Koester, Y.F. Chen, C.K. Clutinger, X.T. Tigno, B.C. Hansen, A.B. Shanafelt, G.J. Etgen, The metabolic state of diabetic monkeys is regulated by fibroblast growth factor-21, Endocrinology 148 (2007) 774–781.
[12] G. Gaich, J.Y. Chien, H. Fu, L.C. Glass, M.A. Deeg, W.L. Holland, A. Kharitonenkov, T. Bumol, H.K. Schilske, D.E. Moller, The effects of LY2405319, an FGF21 analog, in obese human subjects with type 2 diabetes, Cell Metab. 18 (2013) 333–340.
[13] T. Aoyama, J.M. Peters, N. Iritani, T. Nakajima, K. Furihata, T. Hashimoto, F.J. Gonzalez, Altered constitutive expression of fatty acid-metabolizing enzymes in mice lacking the peroxisome proliferator-activated receptor alpha (PPARalpha), J. Biol. Chem. 273 (1998) 5678–5684.
[14] T. Inagaki, P. Dutchak, G. Zhao, X. Ding, L. Gautron, V. Parameswara, Y. Li, R. Goetz, M. Mohammadi, V. Esser, J.K. Elmquist, R.D. Gerard, S.C. Burgess, R.E. Hammer, D.J. Mangelsdorf, S.A. Kliewer, Endocrine regulation of the fasting response by PPARalpha-mediated induction of fibroblast growth factor 21, Cell Metab. 5 (2007) 415–425.
[15] T. Wang, Y.M. Shah, T. Matsubara, Y. Zhen, T. Tanabe, T. Nagano, S. Fotso, K.W. Krausz, T.M. Zabriskie, J.R. Idle, F.J. Gonzalez, Control of steroid 21-oic acid synthesis by peroxisome proliferator-activated receptor alpha and role of the hypothalamic-pituitary-adrenal axis, J. Biol. Chem. 285 (2010) 7670–7685.
[16] M.K. Badman, P. Pissios, A.R. Kennedy, G. Koukos, J.S. Flier, E. Maratos-Flier, Hepatic fibroblast growth factor 21 is regulated by PPARalpha and is a key mediator of hepatic lipid metabolism in ketotic states, Cell Metab. 5 (2007) 426–437.
[17] H.A. Cyphert, X. Ge, A.B. Kohan, L.M. Salati, Y. Zhang, F.B. Hillgartner, Activation of the farnesoid X receptor induces hepatic expression and secretion of fibroblast growth factor 21, J. Biol. Chem. 287 (2012) 25123–25138.
[18] H.A. Cyphert, K.M. Alonge, S.M. Ippagunta, F.B. Hillgartner, Glucagon stimulates hepatic FGF21 secretion through a PKA- and EPAC-dependent posttranscriptional mechanism, PLoS One 9 (2014) e94996.
[19] S.A. Kliewer, D.J. Mangelsdorf, Fibroblast growth factor 21: from pharmacology to physiology, Am. J. Clin. Nutr. 91 (2010) 254S–257S.
[20] D. Ye, Y. Wang, H. Li, W. Jia, K. Man, C.M. Lo, Y. Wang, K.S. Lam, A. Xu, Fibroblast growth factor 21 protects against acetaminophen-induced hepatotoxicity by potentiating peroxisome proliferator-activated receptor coactivator protein-1α-mediated antioxidant capacity in mice, Hepatology 60 (2014) 977–989.
[21] K.R. Feingold, C. Grunfeld, J.G. Heuer, A. Gupta, M. Cramer, T. Zhang, J.K. Shigenaga, S.M. Patzek, Z.W. Chan, A. Moser, H. Bina, A. Kharitonenkov, FGF21 is increased by inflammatory stimuli and protects leptin-deficient ob/ob mice from the toxicity of sepsis, Endocrinology 153 (2012) 2689–2700.
[22] B.A. Neuschwander-Tetri, Hepatic lipotoxicity and the pathogenesis of nonalcoholic steatohepatitis: the central role of nontriglyceride fatty acid metabolites, Hepatology 52 (2010) 774–788.
[23] H. Tilg, A.R. Moschen, Evolution of inflammation in nonalcoholic fatty liver disease: the multiple parallel hits hypothesis, Hepatology 52 (2010) 1836–1846.
[24] J.C. Cohen, J.D. Horton, H.H. Hobbs, Human fatty liver disease: old questions and new insight, Science 332 (2011) 1519–1523.
[25] J. Dushay, P.C. Chui, G.S. Gopalakrishnan, M. Varela-Rey, M. Crawley, F.M. Fisher, M.K. Badman, M.L. Martinez-Chantar, E. Maratos-Flier, Increased fibroblast growth factor 21 in obesity and nonalcoholic fatty liver disease, Gastroenterology 139 (2010) 456–463.
[26] Y. Yilmaz, F. Eren, O. Yonal, R. Kurt, B. Aktas, C.A. Celikel, O. Ozdogan, N. Imeryuz, C. Kalayci, E. Avsar, Increased serum FGF21 levels in patients with nonalcoholic fatty liver disease, Eur. J. Clin. Investig. 40 (2010) 887–892.
[27] H. Li, Q. Fang, F. Gao, J. Fan, J. Zhou, X. Wang, H. Zhang, X. Pan, Y. Bao, K. Xiang, A. Xu, W. Jia, Fibroblast growth factor 21 levels are increased in nonalcoholic fatty liver disease patients and are correlated with hepatic triglyceride, J. Hepatol. 53 (2010) 934–940.
[28] H. Li, K. Dong, Q. Fang, X. Hou, M. Zhou, Y. Bao, K. Xiang, A. Xu, W. Jia, High serum level of fibroblast growth factor 21 is an independent predictor of non-alcoholic fatty liver disease: a 3-year prospective study in China, J. Hepatol. 58 (2013) 557–563.
[29] N. Tanaka, S. Takahashi, Z.Z. Fang, T. Matsubara, K.W. Krausz, A. Qu, F.J. Gonzalez, Role of white adipose lipolysis in the development of NASH induced by methionine- and choline-deficient diet, Biochim. Biophys. Acta 1841 (2014) 1596–1607.
[30] N. Tanaka, T. Matsubara, K.W. Krausz, A.D. Patterson, F.J. Gonzalez, Disruption of phospholipid and bile acid homeostasis in mice with nonalcoholic steatohepatitis, Hepatology 56 (2012) 118–129.
[31] P.A. Dutchak, T. Katafuchi, A.L. Bookout, J.H. Choi, R.T. Yu, D.J. Mangelsdorf, S.A. Kliewer, Fibroblast growth factor-21 regulates PPARγ activity and the antidiabetic actions of thiazolidinediones, Cell 148 (2012) 556–567.
[32] T. Matsubara, N. Tanaka, K.W. Krausz, S.K. Manna, D.W. Kang, E.R. Anderson, H. Luecke, A.D. Patterson, Y.M. Shah, F.J. Gonzalez, Metabolomics identifies an inflammatory cascade involved in dioxin- and diet-induced steatohepatitis, Cell Metab. 16 (2012) 634–644.
[33] S.C. Cazanave, N.A. Elmi, Y. Akazawa, S.F. Bronk, J.L. Mott, G.J. Gores, CHOP and AP-1 cooperatively mediate PUMA expression during lipoapoptosis, Am. J. Physiol. Gastrointest. Liver Physiol. 299 (2010) G236–G243.
[34] S.C. Cazanave, J.L. Mott, S.F. Bronk, N.W. Werneburg, C.D. Fingas, X.W. Meng, N. Finnberg, W.S. El-Deiry, S.H. Kaufmann, G.J. Gores, Death receptor 5 signaling promotes hepatocyte lipoapoptosis, J. Biol. Chem. 286 (2011) 39336–39348.
[35] N. Tanaka, S. Takahashi, T. Matsubara, C. Jiang, W. Sakamoto, T. Chanturiya, R. Teng, O. Gavrilova, F.J. Gonzalez, Adipocyte-specific disruption of fat-specific protein 27 causes hepatosteatosis and insulin resistance in high-fat diet-fed mice, J. Biol. Chem. 290 (2015) 3092–3105.
[36] C. Jiang, C. Xie, F. Li, L. Zhang, R.G. Nichols, K.W. Krausz, J. Cai, Y. Qi, Z.Z. Fang, S. Takahashi, N. Tanaka, D. Desai, S.G. Amin, I. Albert, A.D. Patterson, F.J. Gonzalez, Intestinal farnesoid X receptor signaling promotes nonalcoholic fatty liver disease, J. Clin. Invest. 125 (2015) 386–402.
[37] E. Karaskov, C. Scott, L. Zhang, T. Teodoro, M. Ravazzola, A. Volchuk, Chronic palmitate but not oleate exposure induces endoplasmic reticulum stress, which may contribute to INS-1 pancreatic beta-cell apoptosis, Endocrinology 147 (2006) 3398–3407.
[38] P. Arner, A. Pettersson, P.J. Mitchell, J.D. Dunbar, A. Kharitonenkov, M. Rydén, FGF21 attenuates lipolysis in human adipocytes - a possible link to improved insulin sensitivity, FEBS Lett. 582 (2008) 1725–1730.
[39] X. Li, H. Ge, J. Weiszmann, R. Hecht, Y.S. Li, M.M. Véniant, J. Xu, X. Wu, R. Lindberg, Y. Li, Inhibition of lipolysis may contribute to the acute regulation of plasma FFA and glucose by FGF21 in ob/ob mice, FEBS Lett. 583 (2009) 3230–3234.
[40] K.L. Donnelly, C.I. Smith, S.J. Schwarzenberg, J. Jessurun, M.D. Boldt, E.J. Parks, Sources of fatty acids stored in liver and secreted via lipoproteins in patients with nonalcoholic fatty liver disease, J. Clin. Invest. 115 (2005) 1343–1351.
[41] B. Emanuelli, S.G. Vienberg, G. Smyth, C. Cheng, K.I. Stanford, M. Arumugam, M.D. Michael, A.C. Adams, A. Kharitonenkov, C.R. Kahn, Interplay between FGF21 and insulin action in the liver regulates metabolism, J. Clin. Invest. 124 (2014) 515–527.
[42] F.M. Fisher, P.C. Chui, I.A. Nasser, Y. Popov, J.C. Cunniff, T. Lundasen, A. Kharitonenkov, D. Schuppan, J.S. Flier, E. Maratos-Flier, Fibroblast growth factor 21 limits lipotoxicity by promoting hepatic fatty acid activation in mice on methionine and choline-deficient diets, Gastroenterology 147 (2014) 1073–1083.
[43] K.T. Ong, M.T. Mashek, S.Y. Bu, A.S. Greenberg, D.G. Mashek, Adipose triglyceride lipase is a major hepatic lipase that regulates triacylglycerol turnover and fatty acid signaling and partitioning, Hepatology 53 (2011) 116–126.
[44] F.G. Schaap, A.E. Kremer, W.H. Lamers, P.L. Jansen, I.C. Gaemers, Fibroblast growth factor 21 is induced by endoplasmic reticulum stress, Biochimie 95 (2013) 692–699.
[45] S. Jiang, C. Yan, Q.C. Fang, M.L. Shao, Y.L. Zhang, Y. Liu, Y.P. Deng, B. Shan, J.Q. Liu, H.T. Li, L. Yang, J. Zhou, Z. Dai, Y. Liu, W.P. Jia, Fibroblast growth factor 21 is regulated by the IRE1α-XBP1 branch of the unfolded protein response and counteracts endoplasmic reticulum stress-induced hepatic steatosis, J. Biol. Chem. 289 (2014) 29751–29765.
[46] C.L. Johnson, J.Y. Weston, S.A. Chadi, E.N. Fazio, M.W. Huff, A. Kharitonenkov, A. Köester, C.L. Pin, Fibroblast growth factor 21 reduces the severity of cerulein-induced pancreatitis in mice, Gastroenterology 137 (2009) 1795–1804.